Results in Engineering 6 (2020) 100142

Contents lists available at ScienceDirect

Results in Engineering

journal homepage: www.editorialmanager.com/rineng/Default.aspx

Nonlinear thermal radiation and entropy generation on steady flow of magneto-micropolar fluid passing a stretchable sheet with variable properties

E.O. Fatunmbi [a,*], A. Adeniyan [b]

[a] Department of Mathematics and Statistics, Federal Polytechnic, Ilaro, Nigeria
[b] Department of Mathematics, University of Lagos, Nigeria

ARTICLE INFO

Keywords:
Entropy generation
Magneto-micropolar fluid
Stretchable sheet
Variable fluid properties

ABSTRACT

Various industrial and engineering operations are accompanied with the phenomena of heating and cooling and in such situations, the construction of relevant thermal devices for use in energy and electronic devices is crucial. For efficient performance of such devices, entropy generation should be reduced in the processes. Hence, this study focuses on the impact of nonlinear thermal radiation with entropy production on the steady flow of magneto-micropolar fluid. The flow is generated by a nonlinear stretchable sheet with the influence of variable fluid properties and convective surface heating condition. The controlling mathematical equations are transmuted from partial to ordinary differential equations by similarity conversion procedures and then numerically integrated using shooting techniques accompanied by Runge-Kutta scheme. The graphs of the main physical quantities affecting the velocity, temperature, entropy generation and Bejan number are displayed and discussed. The comparison of the results revealed good relationship with existing ones in literature in the limiting conditions for special cases. From the analysis, it is found that the growth in the magnitude of Prandtl and Eckert numbers enhance entropy generation while the dominance of viscous and Ohmic heating irreversibility over heat transfer irreversibility is observed with a rise in both parameters due to a decline in Bejan number.

1. Introduction

The attention devoted on research of non-Newtonian fluids by scientists and engineers are on the increase in the recent times because these fluids are practically indispensable in a wide and varied range of engineering and industrial processes. For instance in food processing, crude oil extraction, pharmaceuticals, etc. Unlike Newtonian fluids, which display linear proportionality between the rate of shear strain and shear stress, non-Newtonian fluids typically characterize shear thinning or thickening behaviour and sometimes manifest a yield stress. Due to divergent nature of fluid characteristics, the features of all the non-Newtonian fluids cannot be contained in a single constitutive model, hence, the development of various non-Newtonian fluid models based on different physical characteristics or rheology. These include the micropolar model, Casson, Jeffery, Maxwell Johnson-Segalman fluid model, Ostwald De-Wald power law fluid, Giesekus fluid, etc [1].

Notable among the non-Newtonian fluid models is the micropolar fluid concept invented by Eringen [2] and later extended to thermo-micropolar fluid by Ref. [3]. The micropolar fluid is a sub-class of simple microfluids earlier formulated by Eringen [4]. As reported by Jain and Gupta [5], this class of fluids are characterized by microstructures and rigid, bar-like particles suspended in a viscous medium such as polymeric fluids, liquid crystals, animal blood, suspension solutions, etc. This model couples the field of macro-velocity and microrotation together. The possible areas of applications of these fluids in engineering and industrial processes can be traced to the bio-mechanic and chemical engineering, extrusion of polymer, slurry technologies, synovial lubrication, arterial blood flows, knee cap mechanics, etc [6].

Due to its crucial applications as in textile production, extrusion of plastic sheet and metal, drawing of copper wires, glass blowing, drawing of plastic films and so on, quite a number of researchers have engaged in the investigation of boundary layer flow generated by either linear or nonlinear stretchable sheet. Crane [7] pioneered such study by investigating a closed form analytical solution in two-dimensional linearly stretched sheet in which the velocity is proportional to the distance from a fixed origin. Such problem has since been improved upon by various

* Corresponding author.
E-mail addresses: ephesus.fatunmbi@federalpolyilaro.edu.ng (E.O. Fatunmbi), aadeniyan@unilag.edu.ng (A. Adeniyan).

https://doi.org/10.1016/j.rineng.2020.100142
Received 11 March 2020; Received in revised form 23 May 2020; Accepted 24 May 2020

researchers [8–11] reporting the influences of different parameters under diverse assumptions, boundary conditions and geometries. In practical situations, however, the stretching of the sheet assumes a nonlinear form as studied by Ref. [12–15].

In engineering and industrial processes that involve high temperatures, the fluid physical properties such as the viscosity and thermal conductivity cannot be assumed constant due to the fact that high temperature boosts the transport phenomena owing to a decline in the fluid viscosity across the hydrodynamic boundary layer. This in turn influences the thermal boundary layer and at such the rate of heat transfer is also affected. For a better prediction in such situations, it becomes imperative to investigate the impact of varying viscosity and thermal conductivity with temperature in the flow and thermal fields. Such study finds applications in hot rolling, food processing, process of wire drawing [16].

In this regard, Pal and Mondal [17] discussed the impact of both varying viscosity as well as thermal conductivity in a mixed convection flow of a Newtonian fluid passing a stretchable sheet in a porous medium. Such analysis was also reported by Akinbobola and Okoya [18] on second grade fluid with heat source/sink while Animasaun [19] investigated such on Casson fluid over a sheet which stretches exponentially and Gbadeyan *et al.* [20] examined Casson fluid flow with convective surface boundary heating condition and non-uniform viscosity and thermal conductivity. Besides, various scholars ([21,22]) also addressed fluid flow and heat transfer problems involving temperature-dependent fluid properties under diverse conditions and assumptions. Moreover, when high temperature exists within the flow field, the linear thermal radiation becomes invalid, in such cases, the use of the more general nonlinear thermal radiation becomes indispensable. In view of this, Archana [23] addressed the impact of nonlinear radiation on MHD Casson nanofluid, Hosseinzadeh et al. [24] analyzed such problem on Maxwell fluid while Lakshmi *et al.* [25] carried out such analysis on micropolar fluid.

Meanwhile, these aforementioned reports were done via the first law of thermodynamic ignoring the second law of thermodynamics which corresponds to entropy generation which has been found to be dependable than those of the first law (see Kobo and Makinde [26]). In heat transfer problems, entropy generation measures the irreversibility that occurs in a system through the second law of thermodynamics. It also measures the level of the work destruction that is available in a system. Besides, investigations on entropy production explains the sources through which available energy decays in a system such that those sources can be minimized as to achieve an optimal energy required. Bejan [27,28] pioneered such notion while investigating the transfer of heat and thermal design using the second law of thermodynamics. Thereafter, various authors have been encouraged to carry out such analysis on both Newtonian and non-Newtonian fluids.

Makinde and Eegunjobi [29] analyzed entropy production in MHD Newtonian fluid in porous stretching sheet while Seth et al. [30] discussed such subject on MHD nanofluid flow past a nonlinear stretching sheet whereas Tlili *et al.* [31] conducted a survey on 2D MHD nanofluid flow influenced by non-Rosseland thermal radiation and entropy production via a non-Darcy porous medium. More so, Shit and Mandal [32] surveyed such problem for Casson nanofluid with effect of radiation while Srinivasacharya and Bindu [33] examined the problem with the use of micropolar fluid flowing in a porous pipe with the application of convective boundary condition. Salawu and Fatunmbi [34] applied third grade fluid to investigate the subject of entropy production with variable viscosity and convective cooling in porous medium.

Recently, Salawu and Ogunseye [35] computationally carried out such analysis via shooting technique on Powell-Eyring fluid with varying thermal conductivity in a porous channel whereas [36–38] employed micropolar fluid to tackle irreversibility analysis with the influence of thermal radiation. More so, Haider *et al.* [39] numerically addressed such study on an unsteady exponential stretching surface with slip effects. However, none of these studies has reported on entropy generation for the flow of micropolar fluid being generated by nonlinear stretchable sheet with the impact of nonlinear thermal radiation and varying fluid properties in a porous medium.

Therefore, the aim of this current work is to address the problem of entropy generation for magneto-micropolar fluid flow activated by a nonlinear stretchable sheet being influenced by varying fluid properties, with nonlinear thermal radiation, Joule heating and viscous dissipation effects in a porous medium. The work is numerically carried out with a convective condition at the boundary and a weak concentration of the micro-particles at the surface. To the beat of authors knowledge, this work is unique since it has not been considered before in the literature.

2. Basic assumptions for problem formulation

To formulate the mathematical model that is applicable for this study, it has been assumed that:

- The flow is two-dimensional, incompressible and steady on a flat sheet which is non-permeable but stretches nonlinearly with coordinates (x,y) having corresponding velocity components as (u,v) see (Fig. 1) while the working fluid is an electrically conducting micropolar type in porous medium.
- The $x$axis is along the nonlinearly stretched sheet i. e along the flow direction with $y$axis normal to it. The sheet stretches with a velocity $u = U_w = cx^r$ where $c > 0$ and r is the nonlinear stretching parameter.

The governing equations of the steady flow of magneto-micropolar fluid as well as microrotation, heat transfer taking cognizance of the stated assumptions with the boundary layer approximations and thermodynamic second law are listed as follows [36,41,42].

$$\frac{\partial u}{\partial x}+\frac{\partial v}{\partial y}=0, \tag{1}$$

$$u\frac{\partial u}{\partial x}+v\frac{\partial u}{\partial y}=\frac{1}{\rho_\infty}\frac{\partial}{\partial y}\left(\mu\frac{\partial u}{\partial y}\right)+\frac{\mu_r}{\rho_\infty}\frac{\partial^2 u}{\partial y^2}+\frac{\mu_r}{\rho_\infty}\frac{\partial B}{\partial y}-\left(\frac{\sigma B_0^2}{\rho_\infty}+\frac{\nu_\infty}{K_p}\right)u, \tag{2}$$

$$u\frac{\partial B}{\partial x}+v\frac{\partial B}{\partial y}=\frac{\gamma}{\rho_\infty j}\frac{\partial^2 B}{\partial y^2}-\frac{\mu_r}{\rho_\infty j}\left(2B+\frac{\partial u}{\partial y}\right), \tag{3}$$

$$u\frac{\partial T}{\partial x}+v\frac{\partial T}{\partial y}=\frac{1}{\rho_\infty c_p}\left(k(T)+\frac{16\sigma^\star T^3}{3k^\star k_\infty}\right)\frac{\partial^2 T}{\partial y^2}+\frac{(\mu(T)+\mu_r)}{\rho_\infty c_p}\left(\frac{\partial u}{\partial y}\right)^2+\frac{\sigma B_0^2}{\rho_\infty c_p}u^2+\frac{\nu_\infty}{K_p c_p}u^2, \tag{4}$$

$$S_{gen}=\frac{1}{T^2}\left(k(T)+\frac{16\sigma^\star T^3}{3k^\star k_\infty}\right)\left(\frac{\partial T}{\partial y}\right)^2+\frac{(\mu(T)+\mu_r)}{T}\left(\frac{\partial u}{\partial y}\right)^2+\frac{\sigma B_0^2}{T}u^2+\frac{\mu_\infty}{K_p T}u^2. \tag{5}$$

The relevant boundary conditions for this study are as follows:

$$u=U_w=cx^r, v=0, B=-p\frac{\partial u}{\partial y}, -k_\infty\frac{\partial T}{\partial y}=h_f\left(T_f-T\right)aty=0,$$
$$u\to 0, B\to 0, T\to T_\infty \; as \; y\to\infty. \tag{6}$$

The deviation of the micropolar fluid model from the classical Newtonian fluid can be measured by the size of the vortex viscosity parameter μ_r, thus, when $\mu_r = 0$, Eqs. (2) and (4) are decoupled from Eq. (3) and at such, the model under investigation with the results obtained relates to that of Newtonian fluid model. Similarly, the range of validity of the surface boundary parameter $p$is $0 \le p \le 1$, the electric conductivity is assumed to be $\sigma = \sigma_0 x^{r-1}$while $K_p$is a function of $x$given as $K_p = K_p^\star x^{1-r}$and the heat transfer coefficient $h_f = h_1 x^{(r-1)/2}$[43]. It is pertinent also to note that the nonlinear stretching parameter $r = 0$ mirrors uniformly moving sheet while $r = 1$ corresponds to linearly stretching sheet

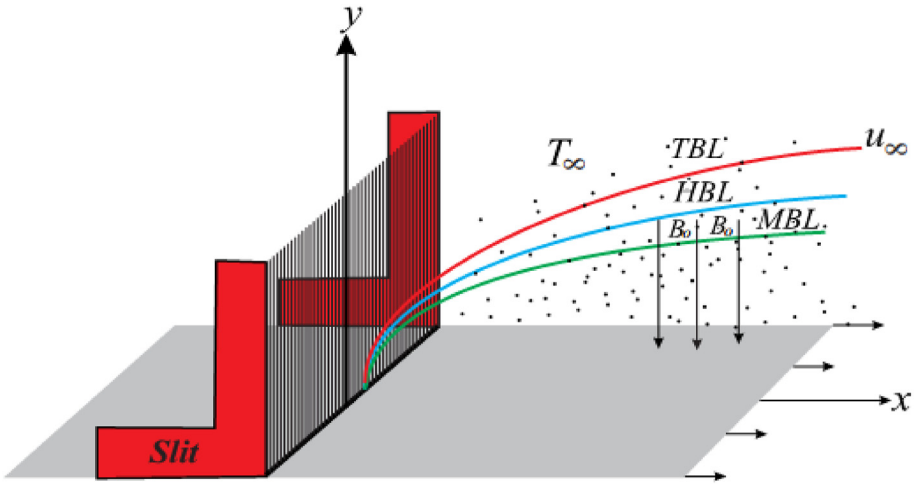

Fig. 1. The sketch of the physical model.

- A uniform external magnetic field $B_o$is normal to the flow direction while the induced magnetic field is not taking into cognizance due to sufficiently low magnetic Reynolds number.
- The radiative heat flux in x-direction is negligible compared to y-direction. The temperature difference within the micropolar fluid layer is not sufficiently small, hence, nonlinear Rosseland approximation (Makinde et al. [40]) in an optically dense opaque medium is applied. The radiative heat flux is given as $q_r = -\frac{4\sigma^*}{3k^*}\frac{\partial T^4}{\partial y}$such that $\frac{\partial q_r}{\partial y} = \frac{\partial}{\partial y}\left(\frac{4\sigma^*}{3k^*}4T^3\frac{\partial T}{\partial y}\right)$.
- The dynamic fluid viscosity is inversely related to temperature while the thermal conductivity vary linearly with it as respectively expressed in Eqs. (7) and (8). The temperature of the sheet is upheld by a convective heating from a hot fluid having temperature $T_f$with a convection heat transfer coefficient $h_f$while the working fluid temperature is below boiling point.
- A finite size control volume at an arbitrary point in a two dimensional convection flow field is assumed for the entropy generation in Eq. (5) with the use of second law of thermodynamics [36].

and $r > 1$ portrays nonlinearly stretching sheet.

The variation of the viscosity with temperature is described in Eq. (7) as [44,45].

$$\frac{1}{\mu} = \frac{1}{\mu_\infty}[1 + \beta(T - T_\infty)] = \zeta(T - T_r), \tag{7}$$

where $\zeta = \frac{\beta}{\mu_\infty}, T_r = T_\infty - \frac{1}{\beta}$. Here, βrelates to the fluid thermal property while $\zeta$and $T_r$remain constants. In the like manner, the micropolar fluid thermal conductivity is assumed to vary in the linear form as [45,46].

$$k(T) = k_\infty\left(1 + \delta\frac{T - T_f}{T_f - T_\infty}\right), \tag{8}$$

where the varying thermal conductivity is symbolized by δ and k_∞ denotes the free stream thermal conductivity. The quantities in Eq. (9) are employed to transmute Eqs. (1)–(6) into ODEs [12–14].

$$\eta = y\left[\frac{c(r+1)x^r}{2x\nu_\infty}\right]^{1/2}, \psi = x^{(r+1)/2}\left[\frac{2\nu_\infty c}{(r+1)}\right]^{1/2} f(\eta), u = \frac{\partial\psi}{\partial y}, B = x^{(3r-1)/2}\left[\frac{c^3(r+1)}{2\nu_\infty}\right]^{1/2} g(\eta)$$
$$v = -\frac{\partial\psi}{\partial x}, \theta(\eta) = \frac{T - T_\infty}{T_f - T_\infty} = \frac{T - T_r}{T_f - T_\infty} + Q, Q = \frac{T_r - T_\infty}{T_f - T_\infty}, j = \left(\frac{\nu}{c}\right)x^{(1-r)}, \gamma = \left(\mu(T) + \frac{\mu_r}{2}\right)j. \tag{9}$$

On substituting Eq. (9) into the governing Eqs. (1)–(6), the continuity Eq. (1) attains validity. Besides, cognizance of Eqs. (7) and (8) the governing Eqs. (2)–(5) yield the underlisted ODEs:

$$\left(\frac{Q}{Q-\theta} + K\right)f''' + ff'' + Kg' + \frac{Q}{(Q-\theta)^2}\theta' f'' - \left(\frac{2r}{r+1}\right)f'^2 - \left(\frac{2}{r+1}\right)(M + Da)f' = 0, \tag{10}$$

$$\left(\frac{Q}{Q-\theta} + K\Big/2\right)g'' + fg' - \left(\frac{3r-1}{r+1}\right)f'g - (2g + f'')\left(\frac{2K}{r+1}\right) = 0, \tag{11}$$

$$\left[1 + \delta\theta + Nr(1 + (\theta_w - 1)\theta)^3\right]\theta'' + 3Nr(\theta_w - 1)\theta'^2(1 + (\theta_w - 1)\theta)^2 + \delta\theta'^2 + Prf\theta' + \left(\frac{Q}{Q-\theta} + K\right)PrEcf''^2 + \left(\frac{2}{r+1}\right)(M + Da)f'^2 = 0. \tag{12}$$

The conditions at the boundary also become

$$\eta = 0 : f' = 1, f = 0, g = -pf'', \theta' = -\alpha(1 - \theta),$$
$$\eta \to \infty : f' = 0, g = 0, \theta = 0. \tag{13}$$

The non-dimensional form of the entropy generation Eq. (6) with $r = 1$ translates to

$$Ns = \frac{1}{(\theta+\Omega)^2}\left[1+\delta\theta+Nr\left(1+(\theta_w-1)\theta\right)^3\right]\theta'^2 + \frac{EcPr}{(\theta+\Omega)}\left(\frac{Q}{Q-\theta}+K\right)f''^2 + \frac{EcPr}{(\theta+\Omega)}(M+Da)f'^2, \tag{14}$$

The sources of entropy production in Eq. (5 or 14) includes: (i) Heat Transfer Irreversibility (HTIR) or the conduction effect indicated by the first term on the right hand side, (ii) Fluid Friction Irreversibility (FFIR) described by the second term and (ii) the combined influence of Magnetic and Darcy Force Irreversibility (MDFIR) is denoted by the third term of Eq. (14). Another important irreversibility distribution measure which of interest to engineers is known as the Bejan number *Be*. It provides an information on which irreversibility source is important and dominating others in the system. It is defined as the ratio of entropy production due to heat transfer to the overall entropy generation. Hence, the Bejan number *Be*can be described as

$$Be = \frac{HTIR}{Ns} = \frac{HTIR}{HTIR+FFIR+MDFIR}, \tag{15}$$

or

$$Be = \frac{\left(1+\delta\theta+Nr(1+(\theta_w-1)\theta)^3\right)\theta'^2(\theta+\Omega)^{-2}}{1+\delta\theta+Nr(1+(\theta_w-1)\theta)^3\theta'^2(\theta+\Omega)^{-2}+EcPr(\theta+\Omega)^{-1}\left[\left(\frac{Q}{Q-\theta}+K\right)f''^2+(M+Da)f'^2\right]}, \tag{16}$$

The incorporated terms/parameters appearing in Eqs. (10)–(14), (16) are designated in Eq. (17) as:

$$M = \frac{\sigma_0 B_o^2}{c\rho_\infty}, Nr = \frac{16T_\infty^3\sigma^\star}{3k^\star k_\infty}, Q = -\frac{1}{\beta(T_f-T_\infty)}, K = \frac{\mu_r}{\mu_\infty}, Pr = \frac{\mu_\infty c_p}{k_\infty}, Ns = \frac{S_{gen}}{S_{gc}}$$

$$Ec = \frac{U_w^2}{c_p(T_w-T_\infty)}, \alpha = \frac{h_1}{k_\infty}\sqrt{\frac{2}{c(r+1)}}, S_{gc} = \frac{ck_\infty}{\nu_\infty}, \Omega = \frac{T_\infty}{(T_w-T_\infty)}, \theta_w = \frac{T_w}{T_\infty}. \tag{17}$$

The various symbols incorporated into the governing equations are listed in Table 1.

3. Numerical method and its validation

The numerical solution for the current study has been carried out by a means of a computer algebra symbolic Maple 2016 package. This has been applied in solving Eqs. (10)–(12) and (14) and (16) together with the accompanied boundary conditions (13). The numerical procedure is rooted in the fourth order Runge-Kutta techniques associated with the shooting scheme. To check the authenticity of the numerical code developed for the governing equations in this work, the computational values obtained for some parameters have been validated with related published works in the literature as relates to the Nusselt number $Nu_x$and coefficient of the skin friction C_{fx}in the limiting cases. Table 2 describes the comparison of computational values of $Nu_x$with those reported by Cortell [12] and Waqas et al. [14] for changes in the Eckert number *Ec*and the nonlinear stretching parameter *r*when $Pr = 1.0$ with $Q \to \infty$and in the absence of $Da, K, M,$ and R. It is remarked that there exists a good relationship between the comparison. Moreover, it is conspicuously shown that growing values of both *Ec*and *r*diminish the rate of heat transfer at the sheet surface as noticed from this table.

Meanwhile, Table 3 depicts the computational values of C_{fx}as compared with the data reported by Lu et al. [47] and Waqas [14] for varying the nonlinear stretching parameter *r*when $Q \to \infty$and $K = 0 = M = Ec = Nr = Da$. An excellent agreement also exists between the values obtained in this work with those authors in the limiting conditions.

Besides the tabular comparisons made in Tables 2 and 3, the variations of velocity profiles $f'(\eta)$ and that of surface temperature distribution $\theta(\eta)$in the absence of porous medium, radiation parameter, thermal conductivity term and for uniform viscosity have been graphically compared with the results of [14]. The results agree well as shown in Figs. 2 and 3. In addition to those parameters absent in Ref. [14], the results also in the absence of material term and magnetic field parameter have been plotted with that of [12] for variation in $f'(\eta)$ and $\theta(\eta)$ as displayed in Figs. 4 and 5. In both cases, the graphs reveal a good agreement.

4. Analysis and discussion of results

The impact of some selected controlling physical quantities on the fluid flow, energy transfer and their reactions on entropy generation

Table 1
Parameters and their description.

Symbol	Description	Symbol	Description
T	Fluid temperature	u, v	Velocity components in x, $y$direction
ν_∞	Free stream kinematic viscosity	h_f	Coefficient of heat transfer
ρ_∞	Free stream fluid density	T_f	Surface sheet temperature
μ_∞	Free stream viscosity	U_w	Velocity at the sheet
μ_r	Vortex viscosity	c	Nonlinear stretching rate
σ	Electrical conductivity	j	Micro inertia density
c_p	Specific heat capacity	γ	Spin gradient viscosity
k	Thermal conductivity	T_∞	Temperature at free stream
$\sigma^\star$	Stefan-Boltzmann constant	$k^\star$	Mean absorption coefficient
B_0	Magnetic field strength	σ_0	Constant
K_p	Porous medium Permeability	$K_p^\star, h_1$	Constants
p	Surface boundary parameter	B	Microrotation component
M	Magnetic field parameter	α	Surface convection parameter
K	Material parameter	Ns	Total entropy generation
Pr	Prandtl number	S_{gc}	Characteristics entropy generation
Q	Viscosity variation parameter	Ω	Temperature difference parameter
Ec	Eckert number	Nr	Radiation parameter
Da	Darcy number	θ_w	Wall temperature excess ratio

*Ns*and the Bejan number *Be*are graphically described in Figs. 2–15 with appropriate analysis and discussion. The computational values adopted are: $Q = 3.0, r = K = M = 0.5 = Da = p = \Omega, Ec = 0.1, Nr = 0.3, Pr = 0.72$and $\alpha = 0.3$. Unless otherwise indicated on the plots.

The combined reaction of the material micropolar *K*and the magnetic field terms on the velocity distribution are described in Fig. 6. Here, the

Table 2
Computed values of Nu_xcompared with [12,14] for varying $r$and.$Q \to \infty$

Ec	r	[12]	[14]	Present
0.0	0.2	0.610262	0.6102	0.6101823
	0.5	0.595297	0.5952	0.5951843
	1.5	0.574537	0.5748	0.5747162
	3.0	0.564472	0.5648	0.5647053
	10.0	0.554960	0.5550	0.5549407
1.0	0.2	0.574985	0.5752	0.5752582
	0.5	0.556623	0.5568	0.5566777
	1.5	0.530966	0.5310	0.5309857
	3.0	0.515777	0.5181	0.5053849

Table 3
Computed values of C_{fx}as compared with existing works of [14,47] for variation in $r$when $K = M = 0 = Da = K$and.$Q \to \infty$

r	[47]	[14]	Present
.0	0.627547	0.6276	0.6275058
.2	0.766758	0.7668	0.7667732
.5	0.889477	0.8895	0.8899665
.0	1.000000	1.0000	0.9999999
.5	1.061587	1.0616	1.0615092
.0	1.148588	1.1486	1.1484923
.0	–	1.2349	1.2347739

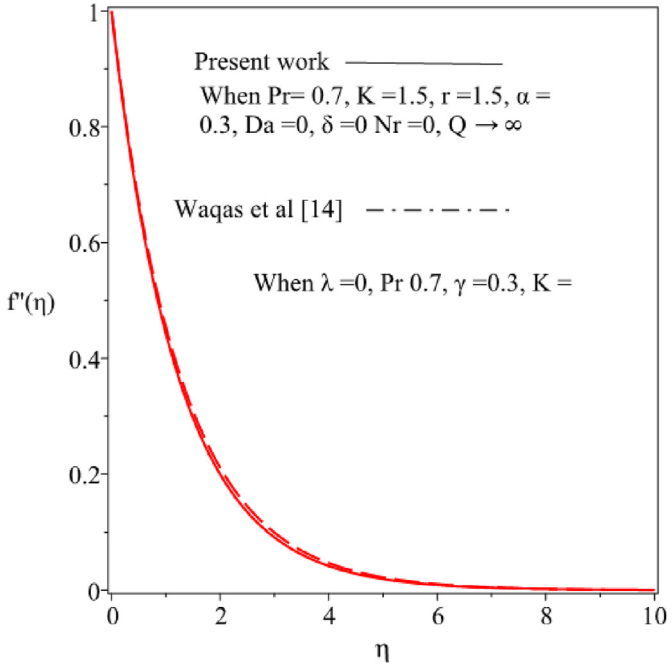

Fig. 2. Velocity profiles.$f'(\eta)$

growth in the material parameter Kthickens the momentum boundary layer and causing the fluid velocity to rise due to reduction in the viscosity. On the contrary, a rise in Mlowers locomotion due to the drag-like magnetic force (Lorentz force) introduced with the application of the magnetic field normal to an electrically conducting micropolar fluid. This force acts against the fluid motion, thereby reducing the velocity. Thus, magnetic field can be employed to control the flow motion which is applicable in areas such as hydromagnetic power generation and electromagnetic coating of wires [48].

Fig. 7 exhibits the response of the temperature profile to variation in the radiation term Nr and M. It is shown that a rise in Nrenhances temperature distribution both in the presence and absence of M. However, the growth in temperature profile is more pronounced when $M$is

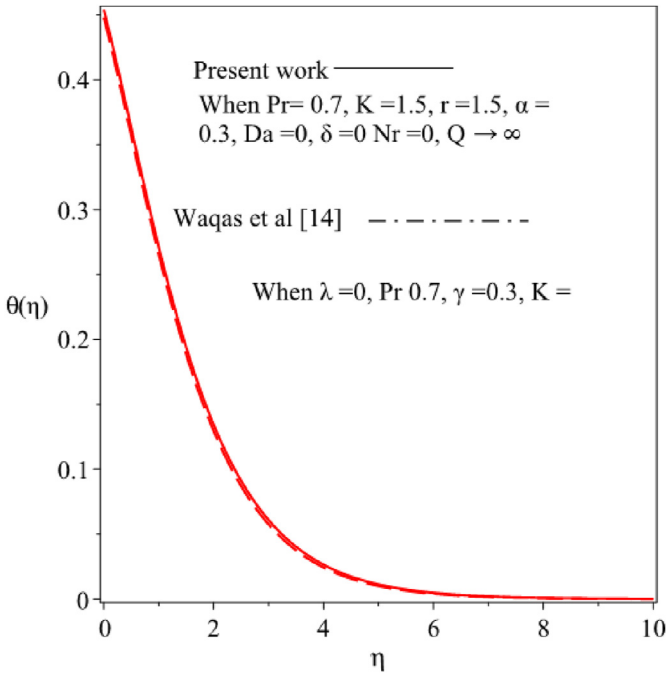

Fig. 3. Temperature $\theta(\eta)$as compared with [14].

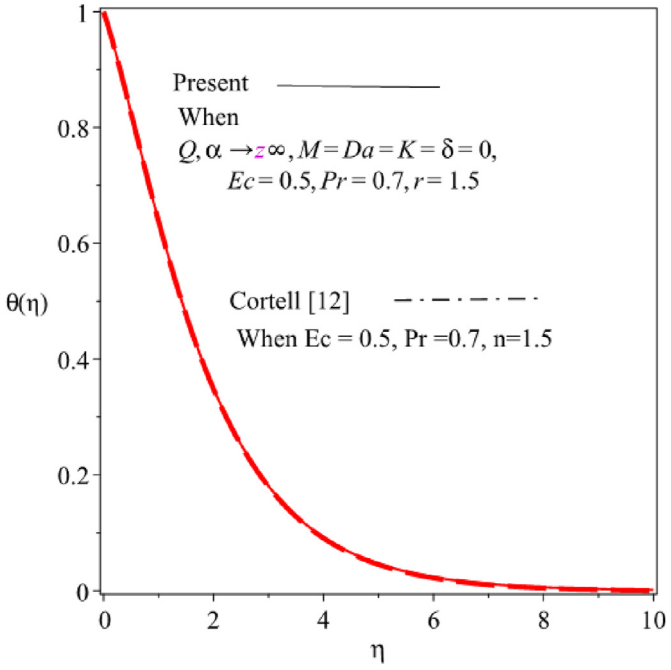

Fig. 4. Comparison of $f'(\eta)$with [12].

present due to an extra heating associated with the imposition of the magnetic field parameter M. Fig. 8 showcases the temperature field constructed against η for variation in the wall temperature excess ratio or heating parameter $\theta_w$in the presence and absence of M. In line with expectation, it evident from this plot that temperature is raised with growing values of $\theta_w$as a result of a rise in the operating temperature difference $T_f - T_\infty$ increases with. θ_w

Fig. 9 shows the sketch of temperature profile against $\eta$for the combined variation of the thermal conductivity $\delta$and Prandtl number Prterms vary. Clearly, a rise in δtends to boost the fluid temperature while

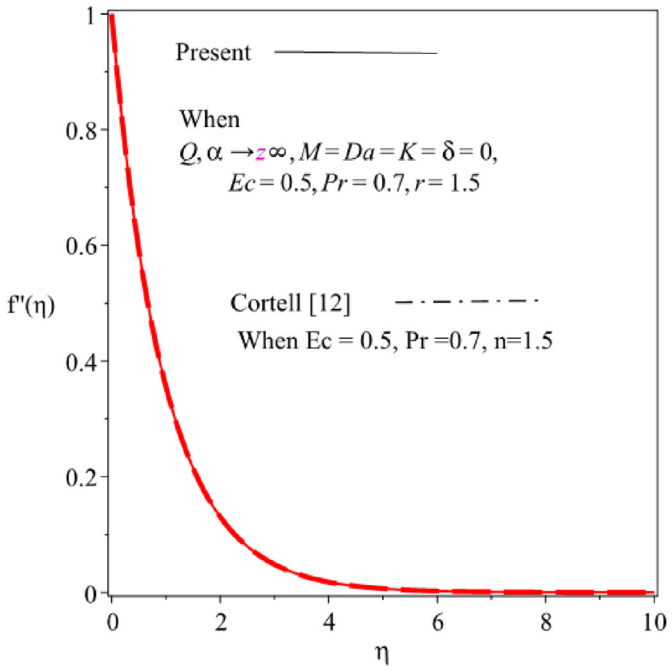

Fig. 5. Comparison of $\theta(\eta)$with [12].

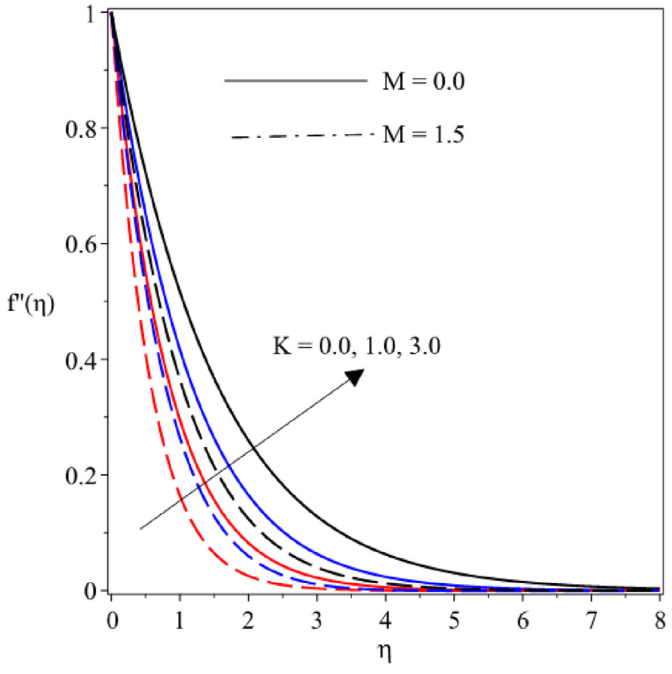

Fig. 6. The velocity field for varying.*K*&*M*

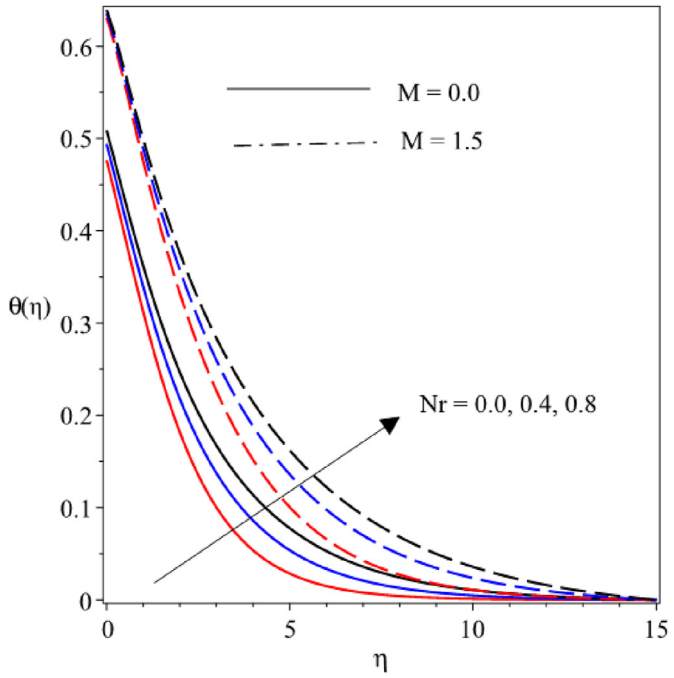

Fig. 7. Impact of *Nr*on temperature.

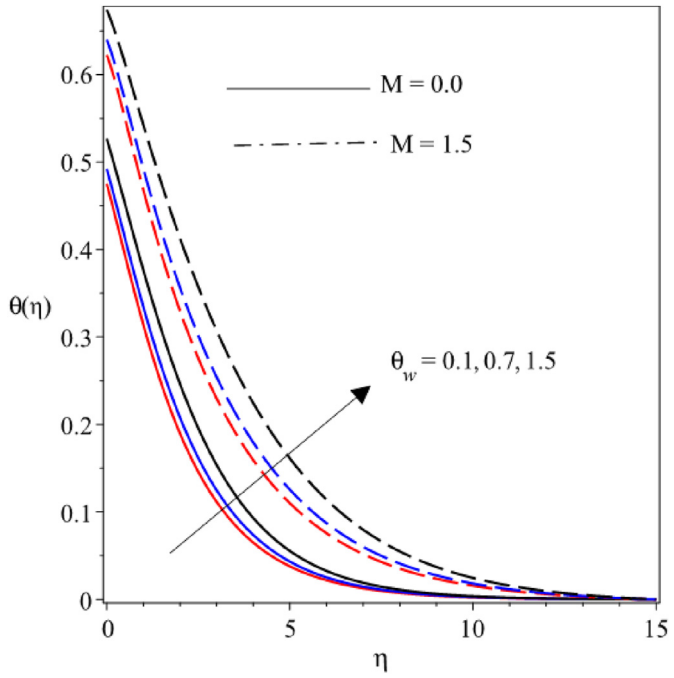

Fig. 8. Temperature field for.θ_w& *M*

*Pr*lowers the temperature distribution due to a decline in the thermal boundary layer thickness. The temperature declines with higher *Pr* due to the fact that fluid with high *Pr* has lower thermal diffusivity and at such, the surface temperature declines. The response of the velocity field to variation in the Darcy number *Da* together with the viscosity variation parameter *Q* is displayed in Fig. 10. The fluid velocity is lowered due to escalating values of *Da* owing to the fact that as the strength of *Da* increases, there is a stronger resistance to the fluid motion. Similarly, it is shown that the fluid velocity is higher for the case of uniform viscosity $Q \to \infty$ whereas the fluid motion decelerates in the presence of *Q* as clearly shown Fig. 10.

Fig. 11 demonstrates the character of the Biot number or surface convection parameter αon the temperature distribution. Evidently, rising values of αencourages the growth of the temperature. Physically, αdefines the ratio of intrinsic thermal resistance of the sheet to that of the boundary layer, hence, a rise in αindicates the dominance of internal heat transfer resistance of the sheet over that of the surface of the sheet. This report is in consonance with that of [14,15].

Figuress 14 and 15 portray the reaction of both *Pr*and *E*con the entropy generation *Ns*as well as on Bejan number *Be*. In Fig. 14, it is shown that the non-dimensional entropy production advances with rising *Pr*. This is so because a rise in *Pr*facilitates higher temperature gradients in the boundary layer and at such, *Ns*is enhanced.

The plot showing the influence of material parameter *K* on entropy

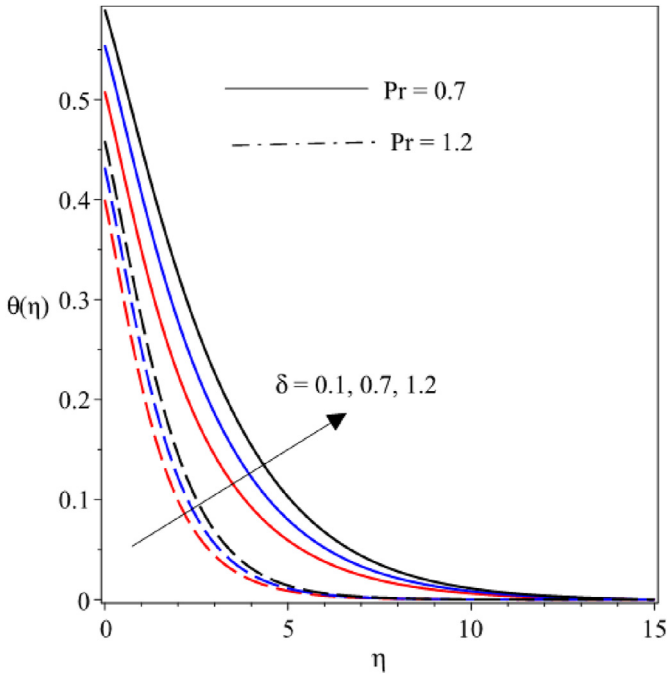

Fig. 9. The reaction of δ & Prwith temperature profile.

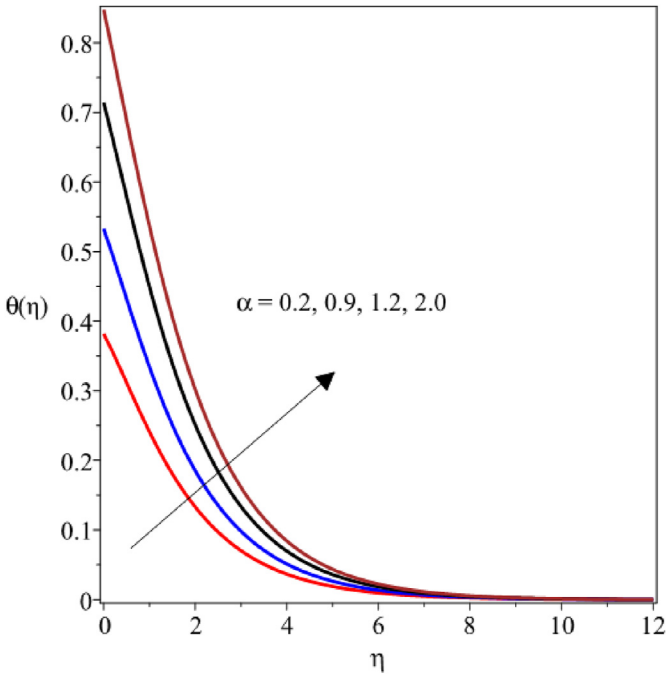

Fig. 11. The reaction of αon temperature.

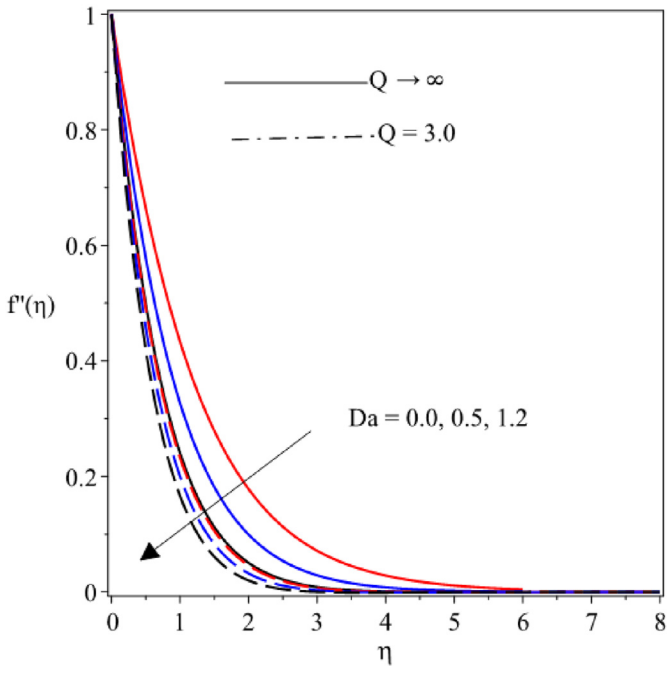

Fig. 10. Response of velocity with.*Da*&*Q*

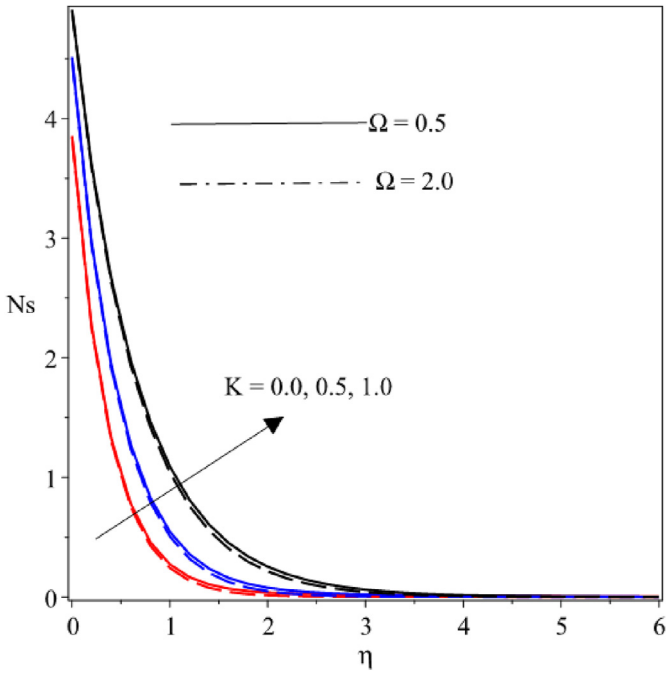

Fig. 12. Impact of *K*&Ωon entropy.*Ns*

generation rates *Ns* is constructed in Fig. 12. With a rise in the magnitude of *K*, there is an increase in the entropy production *Ns*. The strength of the fluid friction and magnetic-Darcy irreversibility over that of heat transfer is observed in Fig. 13 with rising values of *K*. This is so because as *K* rises, the Bejan number *Be* falls irrespective of the value of the temperature difference parameter Ω.

In the like manner, a rise in Eckert number stimulates growth in *Ns*due to the frictional heating effect. This implies that *Ec*should be reduced in order to minimize *Ns*which is the principal aim of the second law of thermodynamics. Both parameters (*Ec*&*Pr*) lower the Bejan number *Be*as showcased in Fig. 15. Observation reveals that for any value of η, the *Be* depreciates with a rise in both *Pr*and *Ec*, the implication of this is that the frictional heating due to viscous dissipation irreversibility and that of the magnetic-Darcy force irreversibility dominate the heat transfer irreversibility.

Figs. 16 and 17 described the effects of wall temperature excess ratio or heating parameter $\theta_w$on both *Ns*and *Be*with changes in dimensionless temperature difference parameter Ω. Rising values in $\theta_w$enhances the production of entropy whereas Ωacts to lower it. In Fig. 17, it is revealed that *Be*rises with an increase in $\theta_w$near the wall but away from it, the trend is reversed. It implies therefore that heat transfer irreversibility is stronger near the stretching sheet with growth in θ_w.

Figs. 18 and 19 showcase how the micropolar material parameter *K*and *M*reacted with the microrotation and temperature profiles. The

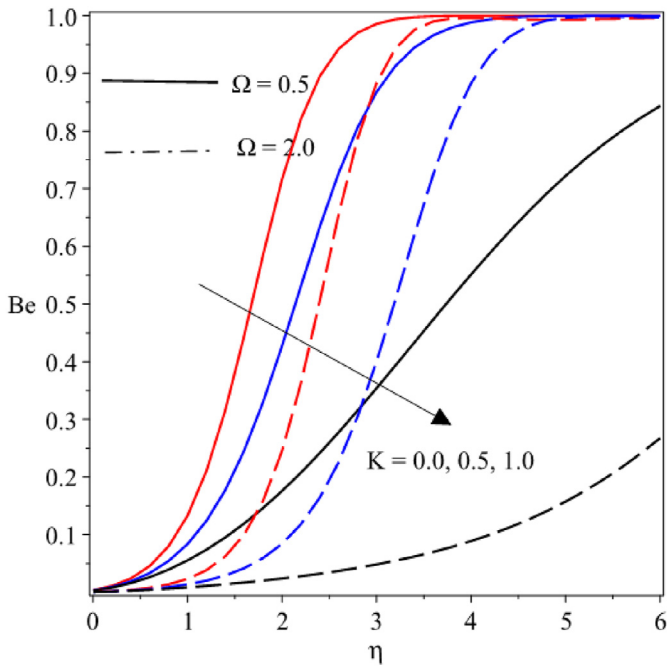

Fig. 13. Reaction of *Be*for changes in.*K*&Ω

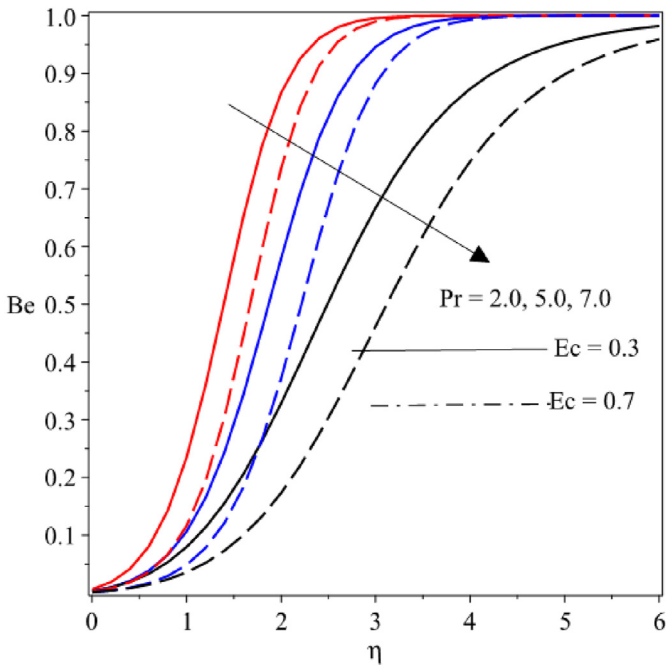

Fig. 15. Benjan number for.*K*

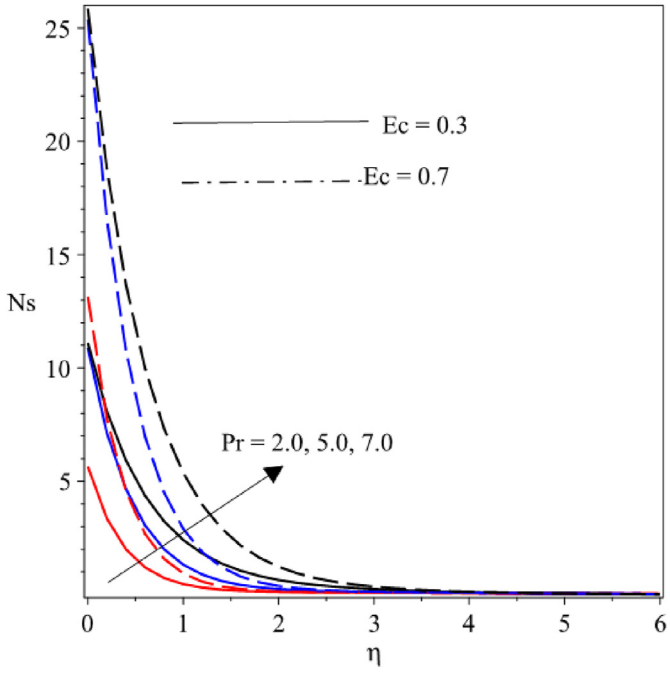

Fig. 14. Entropy generation for material parameter.*K*

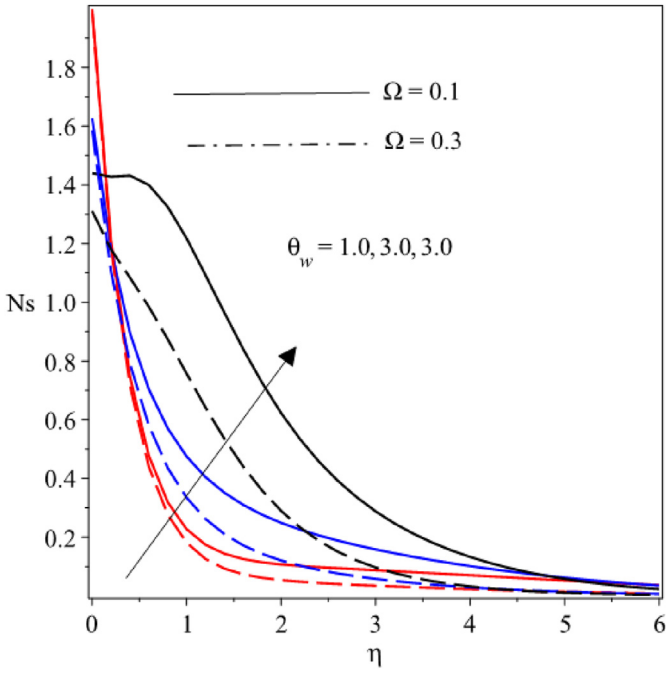

Fig. 16. Entropy generation for radiation parameter.*Nr*

microrotation distribution is seen to decline for growth in the *K*magnitude while the magnetic field parameter facilitates growth in the microrotation distribution. On the other hand, increase in micro-particles as well as application of *M*raises the temperature of the fluid as displayed in Fig. 19.

5. Conclusion

In conclusion, the present study has reported numerically on entropy generation, irreversibility distribution, fluid flow and heat transfer in magneto-magnetic fluid of micropolar type over a nonlinear and non-permeable stretchable sheet. The model has being influenced by variable viscosity and thermal conductivity with the imposition of nonlinear thermal radiation and viscous dissipation among others. The numerical values of some selected parameters gotten from the numerical computation exhibited a good relationship when authenticated by direct comparison with some related existing data available in the literature for limiting situations. From this study, the underlisted points are derived:

- The volumetric rate of entropy generation advances with growing values of material parameter K, heating parameter θ_w, Prandtl $Pr$and Eckert numbers Ecwhereas it declines with growth in the dimensionless temperature difference parameter Ω.

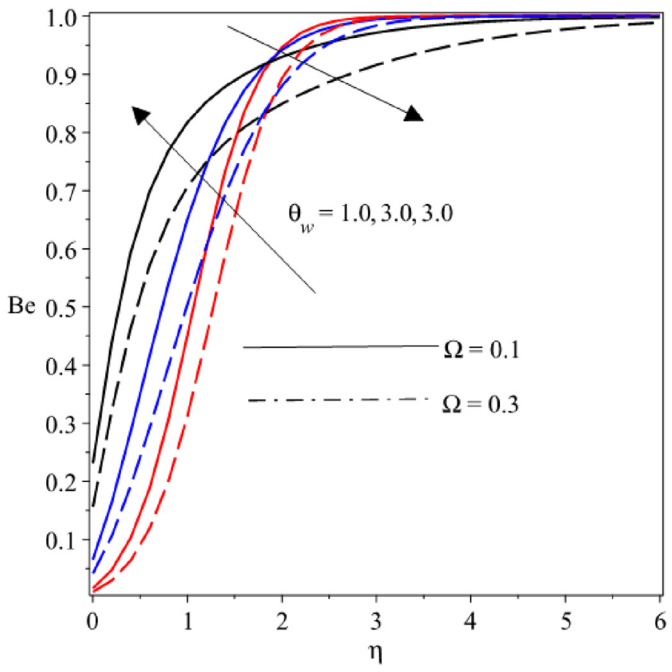

Fig. 17. Bejan number for.*Nr*

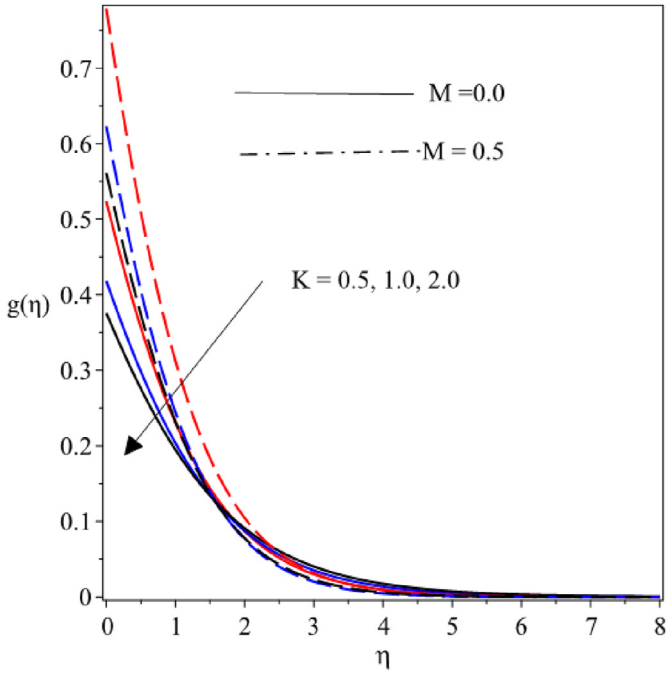

Fig. 18. Impact of *K*on microrotation.

- The heat transfer irreversibility is less important compared to the fluid friction and magnetic-Darcy irreversibility with growth in the material term *K*, Prandtl *Pr*and Eckert numbers *Ec*while such trend is reversed with a rise in heating parameter θ_w.
- The thermal boundary layer becomes thicker and temperature appreciates with rising values of the radiation *Nr*, magnetic field *M*, surface convection α, the micropolar material *K*and the heating parameters $\theta_w$whereas it declines with advancing magnitude of *Pr*.
- The thickness of the momentum boundary layer becomes thin as the magnitude of magnetic field *M*, Darcy number *Da*and the viscosity variation term *Q* advance whereas the opposite occurs with higher values of the material parameter *K*.

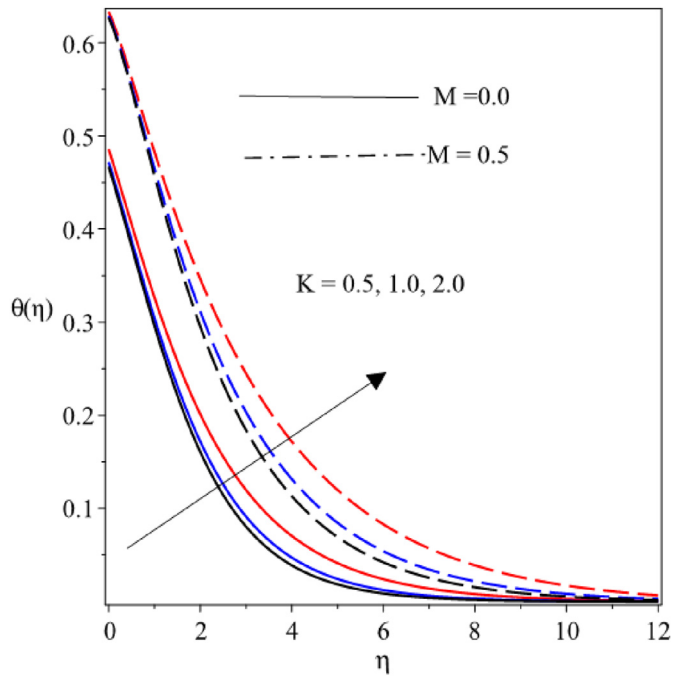

Fig. 19. Influence of *K*on temperature profiles.

Credit author statement

Ephesus Olusoji Fatunmbi: Conceptualization, Methodology, Discussion of Results and Writing the original draft preparation. Adetunji Adeniyan: Result discussions, Supervision, Reading, corrections and Editing.

Authors declaration of conflict of interest

We confirm that the manuscript has been read and approved by all named authors and that there are no other persons who satisfied the criteria for authorship but are not listed. We further confirm that the order of authors listed in the manuscript has been approved by all of us. We confirm that we have given due consideration to the protection of intellectual property associated with this work and that there are no impediments to publication, including the timing of publication, with respect to intellectual property. In so doing we confirm that we have followed the regulations of our institutions concerning intellectual property.

We understand that the Corresponding Author is the sole contact for the Editorial process (including Editorial Manager and direct communications with the office). He is responsible for communicating with the other authors about progress, submissions of revisions and final approval of proofs. We confirm that we have provided a current, correct email address which is accessible by the Corresponding Author and which has been configured to accept email from (ephesus.fatunmbi@federalpolyilaro.edu.ng).

References

[1] E.O. Fatunmbi, S.S. Okoya, Heat transfer in boundary layer magneto-micropolar fluids with temperature-dependent material properties over a stretching sheet, Advances in Materials Science and Engineering (2020) 1–11, 2020.
[2] A.C. Eringen, Theory of micropolar fluids, J. Math. Anal. Appl. 16 (1966) 1–18.
[3] A.C. Eringen, Theory of thermo-microfluids, J. Math. Anal. Appl. 38 (1972) 480–496.
[4] A.C. Eringen, Simple microfluids, Int. J. Eng. Sci. 2 (2) (1964) 205–217.
[5] S. Jain, P. Gupta, Entropy generation analysis of MHD viscoelasticity-based micropolar fluid flow past a stretching sheet with thermal slip and porous media, Int. J. Appl. Comput. Math 1–22 (2019).

[6] Reena, U.S. Rana, Effect of Dust Particles on rotating micropolar fluid heated from below saturating a porous medium, Applications and Applied Mathematics: Int. J. 4 (2009) 189–217.
[7] L.J. Crane, Flow past a stretching plate, Communicatios Breves 21 (1970) 645–647.
[8] H.I. Andersson, Slip flow past a stretching surface, Acta Mech. 158 (2002) 121–125.
[9] L. Kumar, Finite element analysis of combined heat and mass transfer in hydromagnetic micropolar flow along a stretching sheet, Comput. Mater. Sci. 46 (2009) 841–848.
[10] E.O. Fatunmbi, A. Adeniyan, Heat and mass transfer in MHD micropolar fluid flow over a stretching sheet with velocity and thermal slip conditions, Open J. Fluid Dynam. 8 (2018) 195–215.
[11] K. Hsiao, Micropolar nanofluid flow with MHD and viscous dissipation effects towards a stretching sheet with multimedia feature, Int. J. Heat Mass Tran. 112 (2017) 983–990.
[12] R. Cortell, Viscous flow and heat transfer over a nonlinearly stretching sheet, Appl. Math. Comput. 184 (2007) 864–873.
[13] T. Hayat, Z. Abbas, T. Javed, Mixed convection flow of a micropolar fluid over a non-linearly stretching sheet, Phys. Lett. 372 (2008) 637–647.
[14] M. Waqas, M. Farooq, M.J. Khan, A. Alsaedi, T. Hayat, T. Yasmeen, Magnetohydrodynamic (MHD) mixed convection flow of micropolar liquid due to nonlinear stretched sheet with convective condition, Int. J. Heat Mass Tran. 102 (2016) 766–772.
[15] E.O. Fatunmbi, S.S. Okoya, O.D. Makinde, Convective heat transfer analysis of hydromagnetic micropolar fluid flow past an inclined nonlinear stretching sheet with variable thermo-physical properties, Diffus. Found. 26 (2020) 63–77.
[16] T.C. Chiam, Heat transfer in a fluid with variable thermal conductivity over a linearly stretching sheet, Acta Mech. 129 (1998) 63–72.
[17] D. Pal, H. Mondal, Effects of temperature-dependent viscosity and variable thermal conductivity on MHD non-Darcy mixed convective diffusion of species over a stretching sheet, Journal of the Egyptian Mathematical Society (2013) 1–11.
[18] T.E. Akinbobola, S.S. Okoya, The flow of second grade fluid over a stretching sheet with variable thermal conductivity and viscosity in the presence of heat source/sink, Journal of Nigeria Mathematical Society 34 (2015) 331–342.
[19] L.L. Animasaun, E.A. Adebile, A.T. Fagbade, Casson fluid flow with variable thermo-physical property along exponentially stretching sheet with suction and exponentially decaying internal heat generation using the homotopy analysis method, Journal of the Nigerian Mathematical Society (2015) 1–17.
[20] J.A. Gbadeyan, E.O. Titiloye, A.T. Adeosun, Effect of variable thermal conductivity and viscosity on Casson nanofluid flow with convective heating and velocity slip, Heliyon 6 (2020), 1–10.
[21] S.M. Ibrahim, K. Suneetha, Radiation and heat generation effects on steady MHD flow near a stagnation point on a linear stretching sheet in porous medium in presence of variable thermal conductivity and mass transfer, Int. J. Curr. Res. Aca. Rev. 2 (7) (2014) 89–100.
[22] E.O. Fatunmbi, O.J. Fenuga, MHD micropolar fluid flow over a permeable stretching sheet in the presence of variable viscosity and thermal conductivity with Soret and Dufour effects, International Journal of Mathematical Analysis and Optimization: Theory and Applications (2017) 211–232, 2017.
[23] M. Archana, B.J. Gireesha, B.C. Prasannakumara, R.S.R. Gorla, Influence of nonlinear thermal radiation on rotating flow of Casson nanofluid, Nonlinear Eng. (2017) 1–11.
[24] K. Hosseinzadeh, H. Gholinia, B. Jafari, A. Ghanbarpour, H. Olfian, D.D. Ganji, Nonlinear Thermal Radiation and Chemical Reaction Effects on Maxwell Fluid Flow with Convectively Heated Plate in a Porous Medium, Wiley, 2018, pp. 1–11.
[25] R.V. Lakshmi, G. Sarojamma, K. Sreelakshmi, Vajravelu, Transfer Analysis in a micropolar fluid with nonlinear thermal radiation and second-order velocity slip, Applied Mathematics and Scientific Computing (2019) 385–395.
[26] N.S. Kobo, O.D. Makinde, Second law analysis for variable viscosity reactive Couette flow under Arrhenius kinetics, Math. Probl Eng. (2010) 1–15, 2010.
[27] A. Bejan, Second law analysis in heat transfer and thermal design, Adv. Heat Tran. 15 (1982) 1–58.
[28] A. Bejan, Entropy Generation Minimization, second ed., CRC, New York, 1996.
[29] O.D. Makinde, A.S. Eegunjobi, Entropy analysis in MHD flow with heat source and thermal radiation past a stretching sheet in a porous medium, Defect Diffusion Forum 387 (2018) 364–372.
[30] G.S. Seth, A. Bhattacharyya, R. Kumar, A.J. Chamkha, Entropy generation in hydromagnetic nanofluid flow over a non-linear stretching sheet with Navier's velocity slip and convective heat transfer, Phys. Fluids 30 (2018) 1–16.
[31] I. Tlili, M. Ramzan, S. Kadry, H. Kim, Y. Nam, Radiative MHD nanofluid flow over a moving thin needle with entropy generation in a porous medium with dust particles and Hall current, Entropy 22 (2020) 1–17.
[32] G.C. Shit, S. Mandal, Entropy analysis on unsteady MHD flow of Casson nanofluid over a stretching vertical plate with thermal radiation effect, Int. J. Appl. Comput. Math 6 (2) (2020) 1–22.
[33] D. Srinivasacharya, K.H. Bindu, Entropy generation of micropolar fluid flow in an inclined porous pipe with convective boundary conditions, Sadhana 42 (5) (2017) 729–740.
[34] S.O. Salawu, E.O. Fatunmbi, Inherent irreversibility of hydromagnetic Third-grade reactive Poiseuille flow of a variable viscosity in porous media with convective cooling, Journal of the Serbian Society for Computational Mechanics 11 (1) (2017) 46–58.
[35] S.O. Salawu, H.A. Ogunseye, Entropy generation of a radiative hydromagnetic Powell-Eyring chemical reaction nanofluid with variable conductivity and electric field loading, Result in Engineering 5 (2020) 1–8.
[36] M.Y.A. Jamalabadi, Entropy generation in boundary layer flow of a micropolar fluid over a stretching sheet embedded in a highly absorbing medium, Frontier in Heat and Mass Transfer 6 (7) (2015) 1–13.
[37] E.O. Fatunmbi, S.O. Salawu, Analysis of entropy generation in hydromagnetic micropolar fluid flow over an inclined nonlinear permeable stretching sheet with variable viscosity, J. Appl. Comput. Mech. 7 (1) (2021) 1–13.
[38] S.K. Asha, C.K. Deepa, Entropy generation for peristaltic blood flow of a magneto-micropolar fluid with thermal radiation in a tapered asymmetric channel, Result in Engineering 3 (2019) 1–11.
[39] S. Haider, A.S. Butt, Y. Li, S.M. Imran, B. Ahmad, A. Tayyaba, Study of entropy generation with multi-slip effects in MHD unsteady flow of viscous fluid past an exponentially stretching surface, Symmetry 12 (2020) 1–20.
[40] O.D. Makinde, K.G. Kumar, S. Manjunatha, B.J. Gireesha, Effect of nonlinear thermal radiation on MHD boundary layer flow and melting heat transfer of micropolar fluid over a stretching surface with fluid particles suspension, Defect Diffusion Forum 378 (2017) 125–136.
[41] M.I. Afridi, M. Qasim, O.D. Makinde, Minimization of entropy production in three dimensional Dissipative flow of Nanofluid with graphene nanoparticles: a numerical study, Defect Diffusion Forum 387 (2018) 157–165.
[42] J. Qing, M.M. Bhatti, M.A. Abbas, M.M. Rashidi, M.E. Ali, Entropy generation on MHD Casson Nanofluid flow over a porous stretching/shrinking surface, Entropy (2016) 1–10.
[43] A. Ishak, Similarity solutions for flow and heat transfer over a permeable surface with convective boundary condition, Appl. Math. Comput. 217 (2010) 837–842.
[44] A.A. Afify, Effects of variable viscosity on non-Darcy MHD free convection along a non-isothermal vertical surface in a thermally stratified porous medium, Appl. Math. Model. 31 (2007) 1621–1634.
[45] J.X. Ling, A. Dybbs, Forced Convection over a Flat Plate Submersed in a Porous Medium: Variable Viscosity Case, American Society of Mechanical Engineers, 1987, pp. 13–18, 1987.
[46] S.K. Parida, S. Panda, B.R. Rout, MHD boundary layer slip flow and radiative nonlinear heat transfer over a flat plate withvariable fluid properties and thermophoresis, Alexandria Engineering Journal 54 (2015) 941–953.
[47] D. Lu, M. Ramzan, S. Ahmadi, J.D. Chung, U. Farooq, A numerical treatment of MHD radiative flow of micropolar nanofluid with homogeneous-heterogeneous reactions past a nonlinear stretched surface, Sci. Rep. 8 (2018) 1–17.
[48] M. Awais, T. Hayat, A. Ali, S. Irum, Velocity, thermal and concentration slip effects on a magneto-hydrodynamic nanofluid flow, Alexandria Engineering Journal 55 (2016) 2107–2114.